Supplementary Information

A porphyrin-based covalent organic framework with an aminoxyl radical for deep-red light photocatalysis

Keke Zhang‡, Duanfeng Xie‡, Yuexin Wang, Kanghui Xiong, Bo Zhang, Xianjun Lang* and Mian Guo*

Hubei Key Lab on Organic and Polymeric Optoelectronic Materials, College of Chemistry and Molecular Sciences, Wuhan University, Wuhan 430072, China.

**Corresponding authors. E-mail: xianjunlang@whu.edu.cn; whguomian@whu.edu.cn.*

‡*These authors contributed equally to this work.*

Materials and methods

Reagents: Commercially available reagents were purchased from Sigma-Aldrich, TCI, Adamas, etc. All commercially available reagents and solvents were used without further purification.

Fourier transform infrared (FTIR) spectra were recorded from 400 to 4000 cm^{-1} on a Nicolet 5700 FTIR Spectrometer by using KBr pellets.

Solid-state ^{13}C nuclear magnetic resonance (NMR) spectroscopy was utilized to decode the structural information of COFs at the molecular level by using a Bruker AVANCE III HD S6 400MHz NMR spectrometer at room temperature.

^{1}H NMR spectra were recorded at ambient temperature using a Bruker AVANCE II HD (400 MHz) spectrometer. ^{1}H NMR chemical shifts (in ppm) were referenced to chloroform-*d* (δ = 7.26 ppm) as an internal standard.

Nitrogen (N_2) adsorption–desorption isotherms were conducted at 77 K using a Micromeritics ASAP 2460 automated system with the Brunauer–Emmett–Teller (BET) method. The samples were degassed in a vacuum (< 1×10^{-5} bar) at 100 °C for 6 h in the Micromeritics system before N_2 physisorption.

Scanning electron microscopy (SEM) images were measured on a Zeiss Merlin Compact running at an acceleration voltage between 0.1 and 20.0 kV.

Powder X-ray diffraction (PXRD) data were collected at room temperature using a Rigaku/Miniflex 600 diffractometer with a filtered Cu K_α line. Measurements were taken over a 2θ range of 2° to 30°.

Transmission electron microscopy (TEM) of COFs was performed on an FEI Tecnai F20 operating at an accelerating voltage of 200.0 kV.

UV–visible diffuse reflectance spectra (DRS) of COFs were recorded from 300–800 nm by a UV–3600 UV–vis spectrophotometer (Shimadzu, Japan) configured with a diffuse reflectance measurement accessory.

Thermogravimetric analysis (TGA) curves were recorded on an SDT Q600 thermogravimeter from 30 to 800 °C at a rate of 15 ºC min^{-1} under an atmosphere of N_2.

Electron paramagnetic resonance (EPR) spectra were collected on a JEOL JES-FA300 EPR spectrometer.

Periodic density functional theory (DFT) calculations were performed using Vienna ab initio simulation package (VASP) with Perdew-Burke-Ernzerhof (PBE) exchange-correlation functional, and the dispersion interaction was described by the DFT-D3 method. The kinetic energy cut-off for the plane-wave basis was set to 400 eV. A (7×7×1) k-point was used to sample Brillouin zone. During optimization, all atoms were allowed to relax until the residual force was less than 0.02 eV $Å^{-1}$.

Electrochemical measurements: A three-electrode electrochemical cell with an electrochemical workstation was employed to conduct experiments on a Metrohm Autolab PGSTAT302N. At first, the ultrasonic device dispersed 2 mg of COFs in 1 mL of 0.2 wt% Nafion. Subsequently, the mixtures were dripped on glasses coated with indium tin oxide, which were adhered to a glassy carbon surface to serve as the working electrode, and the mixtures were repeatedly dropped and dried under illumination. The Ag/AgCl electrode and platinum wire functioned as the reference electrode and counter electrode, respectively, with 0.1 M Na_2SO_4 aqueous solution as the electrolyte. Meanwhile, the four blue light-emitting diodes (LEDs, 460 nm) positioned at 2 cm from the photoelectrochemical cell were employed as the light source. The photocurrent densities were measured while being exposed to blue LEDs with a scan rate of 100 mV s^{-1} and a time interval of 30 s. In addition, the electrochemical impedance spectroscopy (EIS) was performed in the dark at a bias potential of +1.5 V.

A **gas chromatograph equipped with a flame ionization detector** (GC–FID, Agilent 8890) was employed to confirm the targeted products, sulfoxides, by the retention time in comparison with that of standard samples, using N_2 as the carrier gas and bromobenzene as the internal standard. The products were further verified by gas chromatography–mass spectrometry (GC–MS, Agilent 8890–5977B), using He as the carrier gas.

Conversion of sulfides and selectivity of sulfoxides were defined as follows:

Conv. (%) = $[(C_0 - C_S) / C_0] \times 100$

Sel. (%) = $[C_p / (C_0 - C_S)] \times 100$

where C_0 is the initial concentration of a sulfide, and C_S and C_p are the concentrations of sulfides and sulfoxides, respectively, at a certain time during the reaction.

The procedure of the selective oxidation of sulfide

Primarily, COF (4 mg), methanol (CH_3OH, 1 mL), and sulfide (0.3 mmol) were added to a 10 mL reactor. Then, the reactor was placed in a magnetic stirrer for 15 min to accomplish an adsorption-desorption equilibrium. After exposure to air, the reactor was irradiated by 660 nm red light with constant stirring. Using N_2 as the carrier gas and bromobenzene as the internal standard, the supernatant fluid was analyzed by a GC–FID.

The procedure of cyclic experiments

Upon completion of the reaction, the catalyst was isolated by centrifugation, washed with CH_3OH, and vacuum-dried at 80 °C for 3 h. The dried solid was directly reused in subsequent cycles without further treatment.

Synthesis of 5,10,15,20-tetrakis(4-benzaldehyde)porphyrin (*p*-Por-CHO)

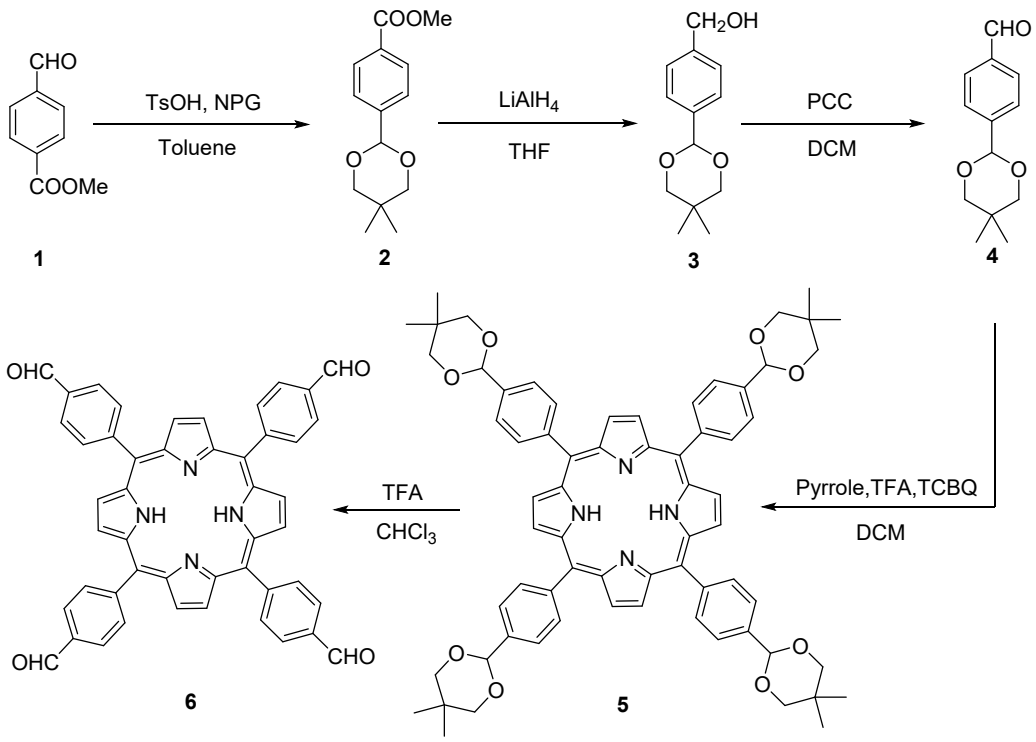

Synthesis of methyl 4-(5,5-dimethyl-1,3-dioxan-2-yl)benzoate (2)

p-Formyl methyl benzoate (10.0 g, 61.0 mmol), neopentyl glycol (NPG, 7.0 g, 67.0 mmol), *p*-toluenesulfonic acid (TsOH, 52.0 mg, 0.3 mmol), and toluene (100 mL) were added to a 250 mL pear-shaped flask. The reaction mixture was heated to reflux after a Dean-Stark apparatus and a reflux condenser were attached. The reaction was continued until no further water was collected in the Dean-Stark trap. After the reaction was completed, the reaction mixture was cooled to room temperature, and the solvent was removed under reduced pressure using a rotary evaporator. The crude product was recrystallized from ethanol. After 24 h, the solid was collected by filtration, washed with a small amount of ethanol, and dried in a vacuum drying oven at 40 °C for 12 h to afford methyl 4-(5,5-dimethyl-1,3-dioxan-2-yl)benzoate as a solid (14.8 g, 97% yield). ^{1}H NMR (400 MHz, Chloroform-*d*) δ 8.05 (d, *J* = 8.0 Hz, 2H), 7.58 (d, *J* = 8.0 Hz, 2H),

5.43 (s, 1H), 3.91 (s, 3H), 3.79 (d, *J* = 8.1 Hz, 2H), 3.66 (d, *J* = 8.1 Hz, 2H), 1.29 (s, 3H), 0.81 (s, 3H).

Synthesis of (4-(5,5-dimethyl-1,3-dioxan-2-yl)phenyl)methanol (3)

Anhydrous THF (80 mL) was added to a 250 mL three-necked round-bottom flask charged with lithium aluminum hydride ($LiAlH_4$, 1.0 g, 26.0 mmol). Under an ice–water bath, a solution of methyl 4-(5,5-dimethyl-1,3-dioxan-2-yl)benzoate (5.0 g, 20.0 mmol) in THF was slowly added dropwise via a pressure-equalizing dropping funnel. After completing the addition, the reaction mixture was allowed to warm to room temperature and stirred for 4–6 h. After completion of the reaction, a 25 *wt*% aqueous NaOH solution was slowly added dropwise under an ice–water bath with continuous stirring until no further gas evolution was observed. The mixture was filtered through diatomaceous earth to remove insoluble materials. The filtrate was concentrated under reduced pressure to afford (4-(5,5-dimethyl-1,3-dioxan-2-yl)phenyl)methanol as a solid (3.9 g, 90% yield). ^{1}H NMR (400 MHz, Chloroform-*d*) δ 7.50 (d, *J* = 8.0 Hz, 2H), 7.34 (d, *J* = 8.0 Hz, 2H), 5.39 (s, 1H), 4.67 (d, *J* = 8.0 Hz, 2H), 3.77 (d, *J* = 12.0 Hz, 2H), 3.65 (d, *J* = 12.0 Hz, 2H), 1.29 (s, 3H), 0.80 (s, 3H).

Synthesis of 4-(5,5-dimethyl-1,3-dioxan-2-yl)benzaldehyde (4)

Dry CH_2Cl_2 (100 mL) was added to a 250 mL three-necked round-bottom flask charged with pyridinium chlorochromate (PCC, 8.8 g, 41.2 mmol), and the mixture was stirred until a homogeneous suspension was formed. A solution of (4-(5,5-dimethyl-1,3-

dioxan-2-yl)phenyl)methanol (6.1 g, 30.0 mmol) in CH_2Cl_2 was then added dropwise via a pressure-equalizing dropping funnel. After complete addition, the reaction mixture was stirred at room temperature for more than 8 h. Upon completion of the reaction, the oily residue was directly loaded onto a silica gel column and purified by column chromatography using CH_2Cl_2 as the eluent to afford 4-(5,5-dimethyl-1,3-dioxan-2-yl)benzaldehyde as a solid (5.6 g, 85% yield). ^{1}H NMR (400 MHz, Chloroform-*d*) δ 10.02 (s, 1H), 7.89 (d, *J* = 8.0 Hz, 2H), 7.68 (d, *J* = 8.0 Hz, 2H), 5.45 (s, 1H), 3.79 (d, *J* = 8.0 Hz, 2H), 3.67 (d, *J* = 8.0 Hz, 2H), 1.29 (s, 3H), 0.81 (s, 3H).

Synthesis of 5,10,15,20-tetrakis(4-(5,5-dimethyl-1,3-dioxan-2-yl)phenyl)porphyrin (5)

4-(5,5-Dimethyl-1,3-dioxan-2-yl)benzaldehyde (11.0 g, 50.0 mmol) was dissolved in CH_2Cl_2 (1000 mL) in a 2000 mL three-necked round-bottom flask under N_2 and avoid light environment. Freshly distilled pyrrole (4.0 mL, 60.2 mmol) was added, and the reaction mixture was stirred at room temperature for 0.5 h. Trifluoroacetic acid (TFA, 2.8 mL, 39.0 mmol) was then added, and the mixture was allowed to react under dark conditions for 2 h. Subsequently, tetrachlorobenzoquinone (TCBQ, 5.9 g, 24.1 mmol) was added, and the reaction mixture was stirred for more than 12 h at room temperature. After completion, the solvent was removed under reduced pressure. The crude product was subjected to short-path column filtration and purified by column chromatography to afford 5,10,15,20-tetrakis(4-(5,5-dimethyl-1,3-dioxan-2-yl)phenyl)porphyrin as a

solid (0.4 g, 1% yield). The low yield is typical for meso-substituted porphyrin condensation. ^{1}H NMR (400 MHz, Chloroform-*d*) δ 8.82 (s, 8H), 8.22 (d, *J* = 8.0 Hz, 8H), 7.91 (d, *J* = 8.0 Hz, 8H), 5.76 (s, 4H), 3.97 (d, *J* = 8.0 Hz, 8H), 3.86 (d, *J* = 8.0 Hz, 8H), 1.47 (s, 12H), 0.92 (s, 12H), −2.86 (s, 2H).

Synthesis of *p*-Por-CHO (6)

$CHCl_3$ (5 mL) and TFA (3 mL, 40.3 mmol) were added to a 50 mL pear-shaped flask containing 5,10,15,20-tetrakis(4-(5,5-dimethyl-1,3-dioxan-2-yl)phenyl)porphyrin (0.5 g, 0.48 mmol). The reaction mixture was stirred at room temperature for 48 h, and the progress of the reaction was monitored by TLC. After completion, a saturated aqueous K_2CO_3 solution was slowly added under an ice–water bath until no further gas evolution was observed. The resulting solid was collected by filtration, washed with ethanol, and dried at 50 °C for 12 h to afford *p*-Por-CHO as a purple solid (334 mg, 96% yield). ^{1}H NMR (400 MHz, Chloroform-*d*) δ 10.40 (s, 4H), 8.83 (s, 8H), 8.40 (d, *J* = 8.0 Hz, 8H), 8.32–8.28 (m, 8H), −2.78 (s, 2H).

Construction of Por-sp^{2}c-COF

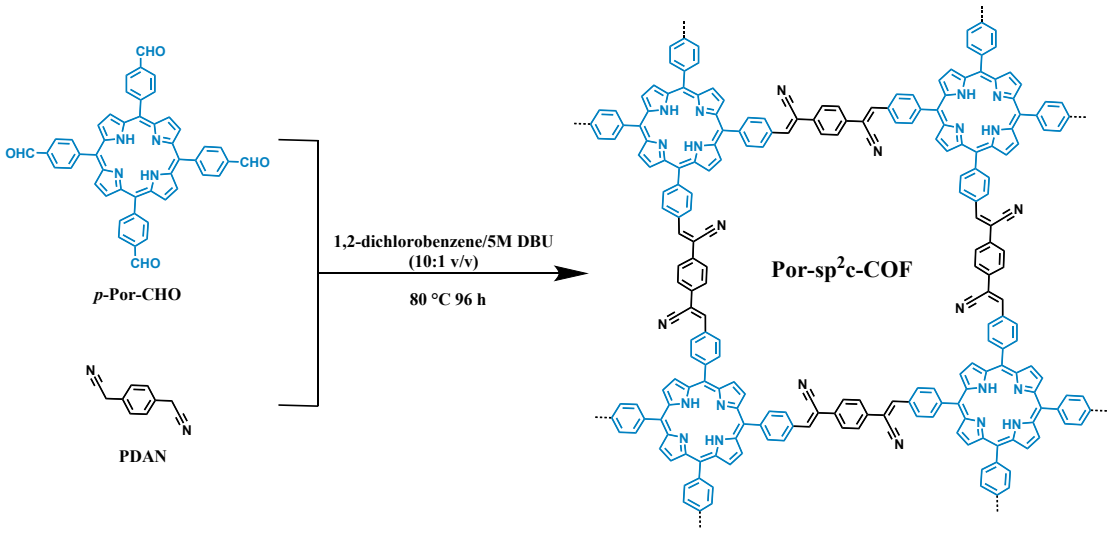

Por-sp^{2}c-COF was constructed according to the reported literature.[1] A Pyrex tube was charged with *p*-Por-CHO (69.72 mg, 0.096 mmol), PDAN (30 mg, 0.192 mmol), 1,2-dichlorobenzene (4 mL) and aqueous DBU solution (0.4 mL, 5 M), the mixture was sonicated for 5 minutes, degassed through three freeze-pump-thaw cycles, sealed under vacuum and heated in an oven at 80 ℃ for 96 h. The mixture was cooled to room temperature, and the precipitate was collected by centrifugation, washed with dichloromethane several times, Soxhlet extracted in tetrahydrofuran and dichloromethane for 2 days, and dried under vacuum at 80 ℃ for 12 h to afford dark purple powder (64.8 mg) in 65% isolated yield.

Supplementary Figures and Tables

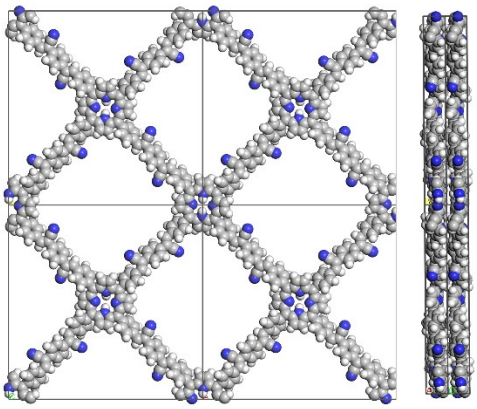

Figure S1. Top and side views of the crystal packing of Por-sp^{2}c-COF showing a [2 × 2 × 1] array of unit cells in a ball-and-stick representation.

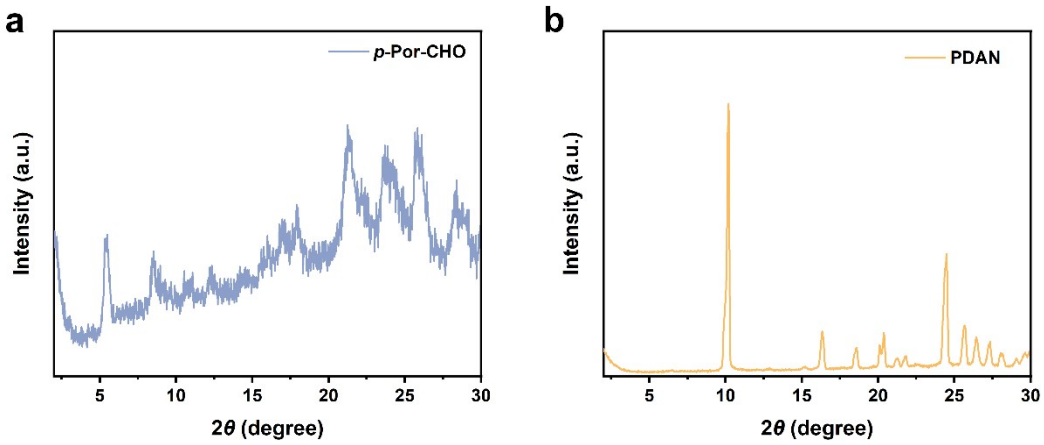

Figure S2. PXRD patterns of *p*-Por-CHO (a) and PDAN (b).

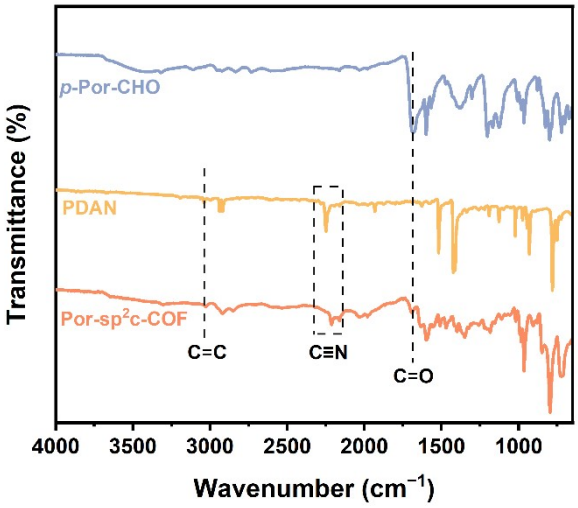

Figure S3. FTIR spectra of Por-sp^{2}c-COF and the building blocks.

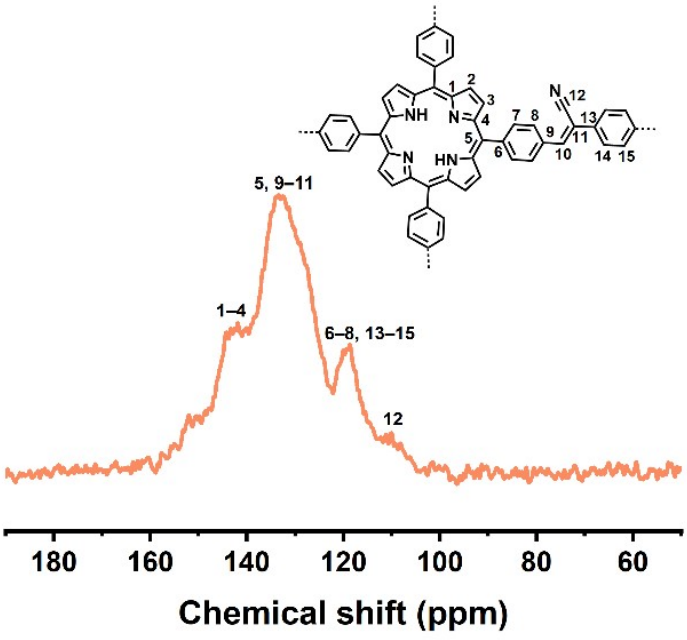

Figure S4. Solid-state ^{13}C NMR spectrum of Por-sp^{2}c-COF.

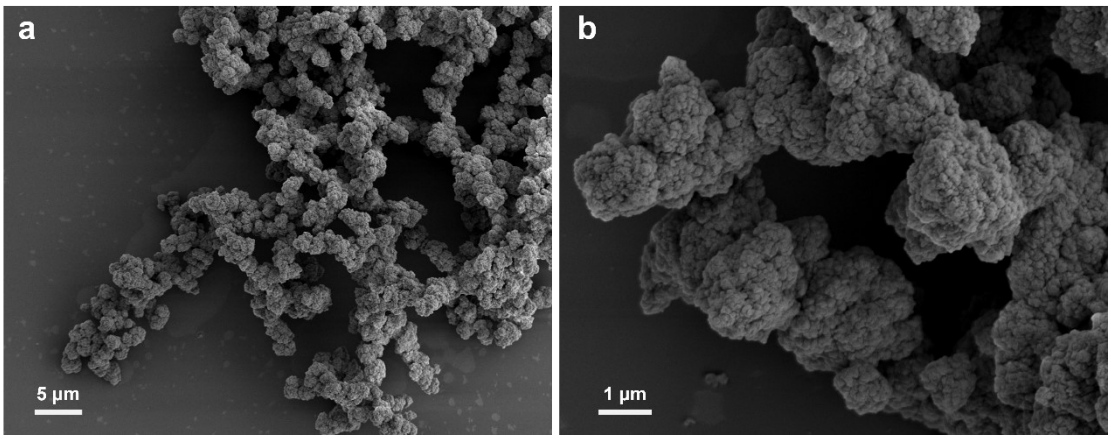

Figure S5. SEM images of Por-sp^{2}c-COF.

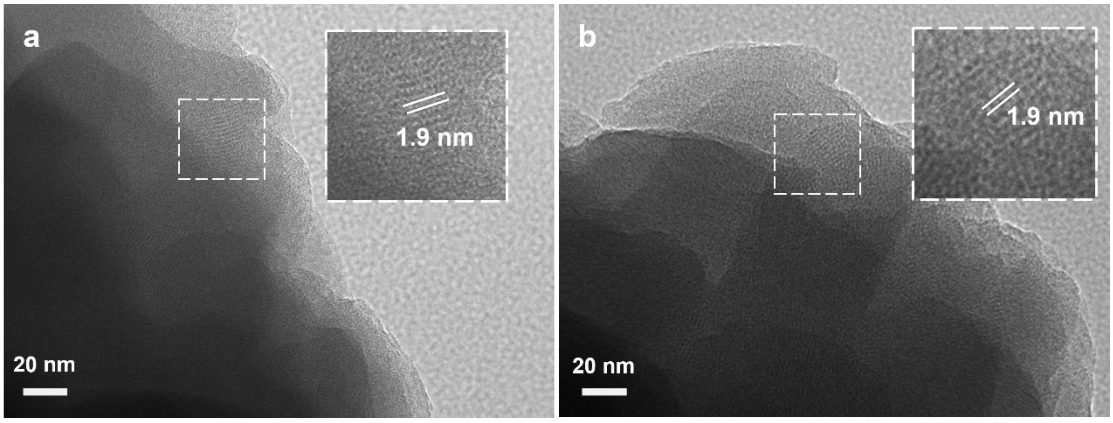

Figure S6. TEM images of Por-sp^{2}c-COF.

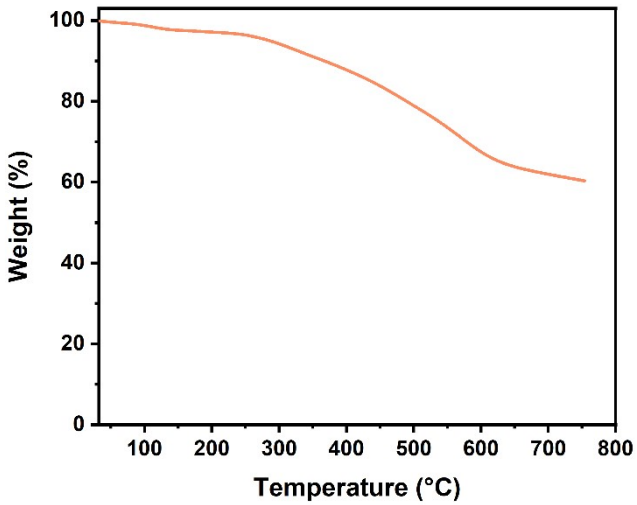

Figure S7. TGA curve of Por-sp^{2}c-COF.

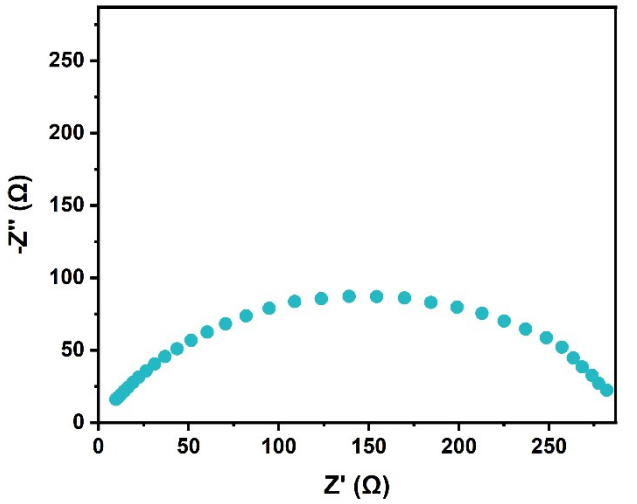

Figure S8. EIS Nyquist plots of Por-sp^{2}c-COF.

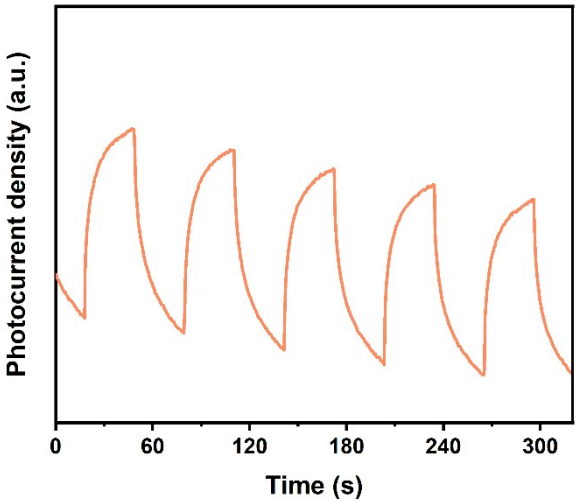

Figure S9. Transient photocurrent response of Por-sp^{2}c-COF.

Table S1. The influence of different solvents on the selective oxidation of sulfide by Por-sp^{2}c-COF/ABNO photocatalysis.[a]

Entry	Solvent	Conv. (%)[b]	Sel. (%)[b]
1	CH_3CN	27	99
2	C_2H_5OH	66	99
3	CH_3OH	83	99

[a] Reaction conditions: sulfide (0.3 mmol), Por-sp^{2}c-COF (4 mg), red light (660 nm), air, 2 mol% ABNO, solvent (1 mL), 25 min.

[b] Determined by GC–FID using bromobenzene as the internal standard.

Table S2. The influence of light sources on the selective oxidation of sulfide by Por-sp^{2}c-COF/ABNO photocatalysis.[a]

Entry	Light	λ_p (nm)	Conv. (%)[b]	Sel. (%)[b]
1	Red	660	41	99
2	Red	620	32	99
3	Yellow	590	5	99
4	Green	520	11	99
5	Blue	460	57	93
6	White	continuous	18	99

[a] Reaction conditions: sulfide (0.3 mmol), Por-sp^{2}c-COF (4 mg), air, 2 mol% ABNO, CH_3OH (1 mL), 12 min.

[b] Determined by GC–FID using bromobenzene as the internal standard.

Table S3. Substrate scope of the selective oxidation of sulfides by Por-sp^{2}c-COF/ABNO photocatalysis at the same time.[a]

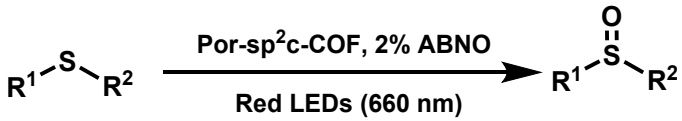

Entry	Substrate	Product	Conv. (%)[b]	Sel. (%)[b]
1	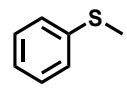	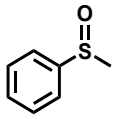	83	95
2	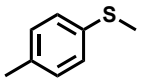	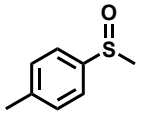	90	95
3	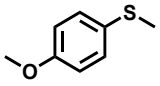	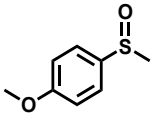	99	95
4	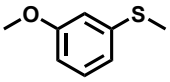	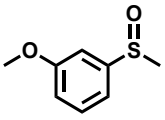	67	94
5	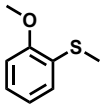	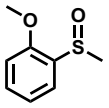	79	99
6	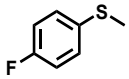	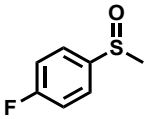	71	95
7	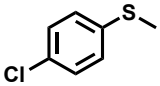	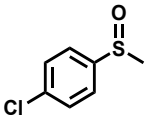	65	94
8	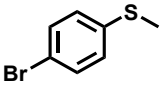	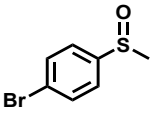	71	93
9	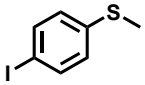	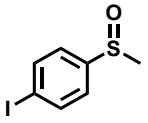	79	92

10	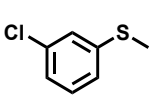	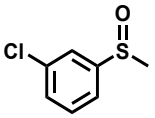	50	93
11	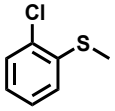	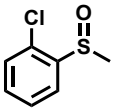	26	99
12	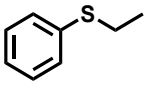	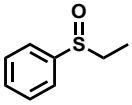	68	94

[a] Reaction conditions: sulfides (0.3 mmol), Por-sp^{2}c-COF (4 mg), red light (660 nm), air, 2 mol% ABNO, CH_3OH (1 mL), 25 min.

[b] Determined by GC–FID using bromobenzene as the internal standard.

Table S4. Comparison of Por-sp^{2}c-COF with previously reported catalysts for the selective oxidation of sulfide.

Entry	Catalyst	Conditions	t (h)	Conv. (%)	Ref.
1	C-CMP (20 mg)	Sulfide (1.0 mmol), CH_3CN (2 mL), Xe lamp (250 W), O_2 (1 atm)	8	99	[2]
2	COF-NUST-31 (4 mg)	Thioanisole (0.1 mmol), CH_3CN (1.5 mL), 30 W blue light (λ = 455–460 nm), O_2 (1 atm)	4	99	[3]
3	BSe-COF (10 mg)	Thioanisole (0.3 mmol), C_2H_5OH (3 mL), 9 W LED lamp (460 nm), O_2	8	95	[4]
4	Zr-MOF-OH (7 mg)	Sulfide (0.2 mmol), CF_3CH_2OH (3.0 mL), white LED (5 W), O_2 (1 atm)	8	99	[5]
5	PW_{12}-Ag@COF (3 mg)	Thioanisole (0.1 mmol), CH_3CN (1.5 mL), 10 W 425 nm LED, O_2 (1 atm)	4	93	[6]
6	Por-sp^{2}c-COF (4 mg)	Thioanisole (0.3 mmol), CH_3OH (1 mL), red light irradiation, air	0.5	92	This work

Table S5. The selective oxidation of sulfide by Por-sp^{2}c-COF/ABNO photocatalysis under diverse controlled conditions.[a]

Entry	Condition	Conv. (%)[b]	Sel. (%)[b]
1	standard	83	99
2	N_2	0	--
3	dark	0	--
4	Without COF	0	--

[a] Reaction conditions: sulfide (0.3 mmol), Por-sp^{2}c-COF (4 mg), red light (660 nm), air, 2 mol% ABNO, CH_3OH (1 mL), 25 min.

[b] Determined by GC–FID using bromobenzene as the internal standard.

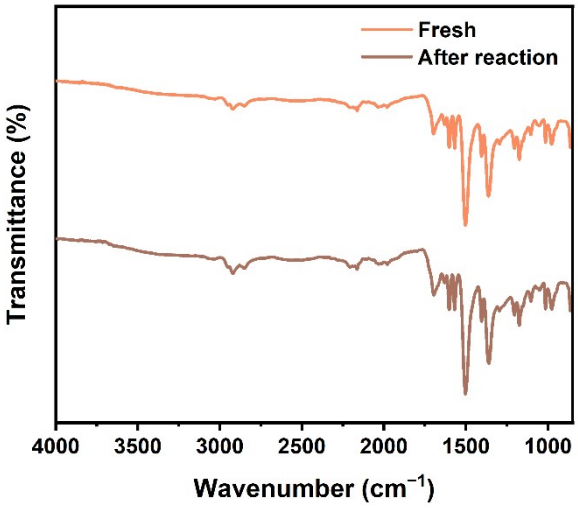

Figure S10. FTIR spectra of the fresh and recovered Por-sp^{2}c-COF.

Figure S11. GC–FID results for Table 1.

Table 1, Entry 1

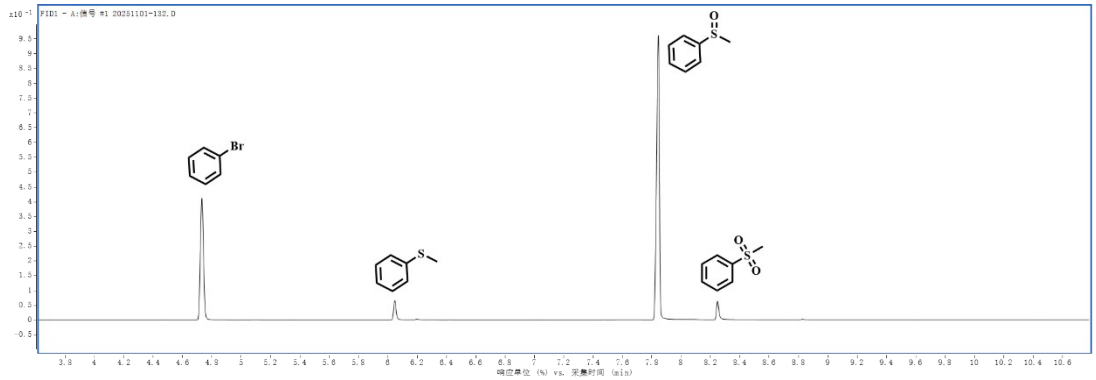

Table 1, Entry 2

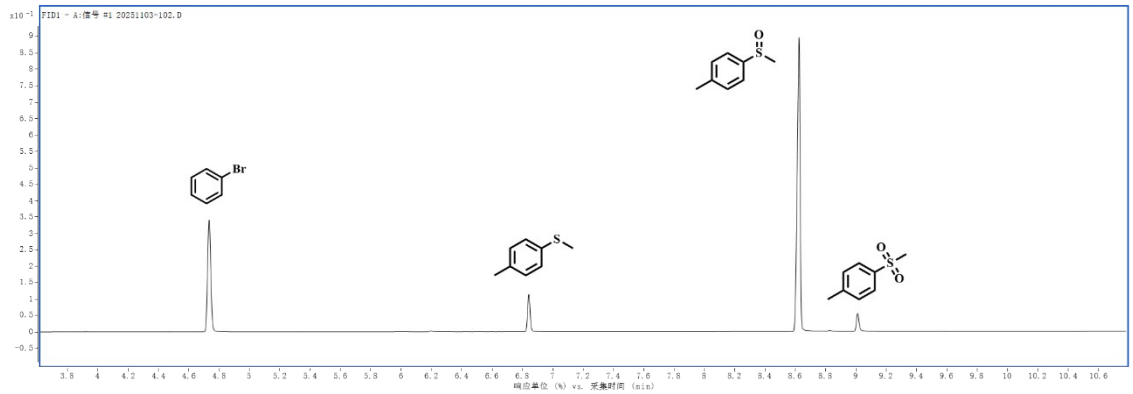

Table 1, Entry 3

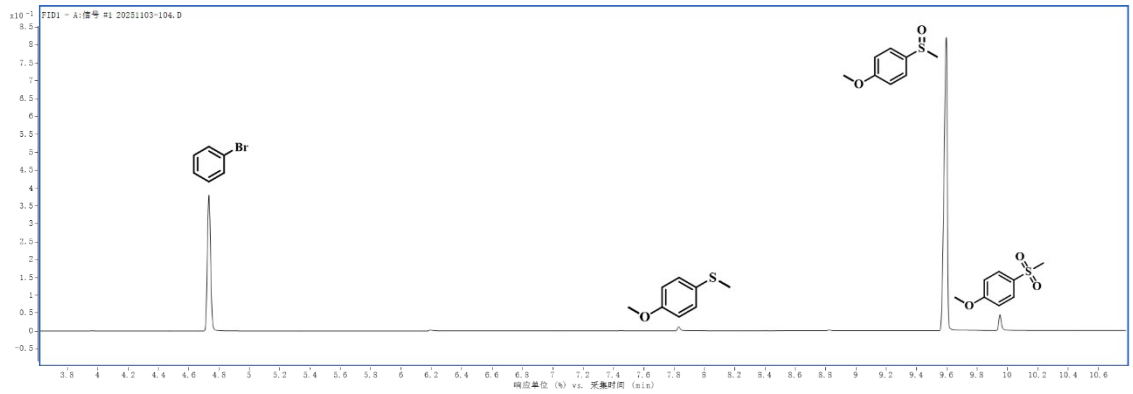

Table 1, Entry 4

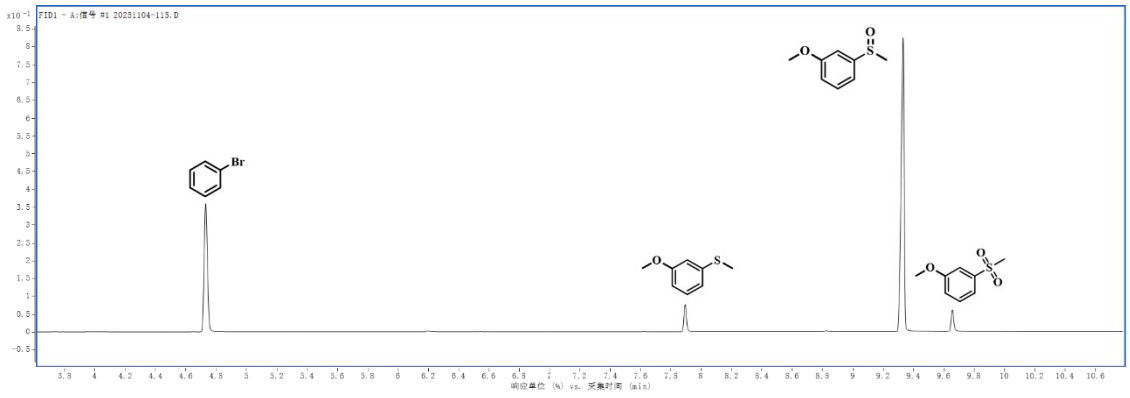

Table 1, Entry 5

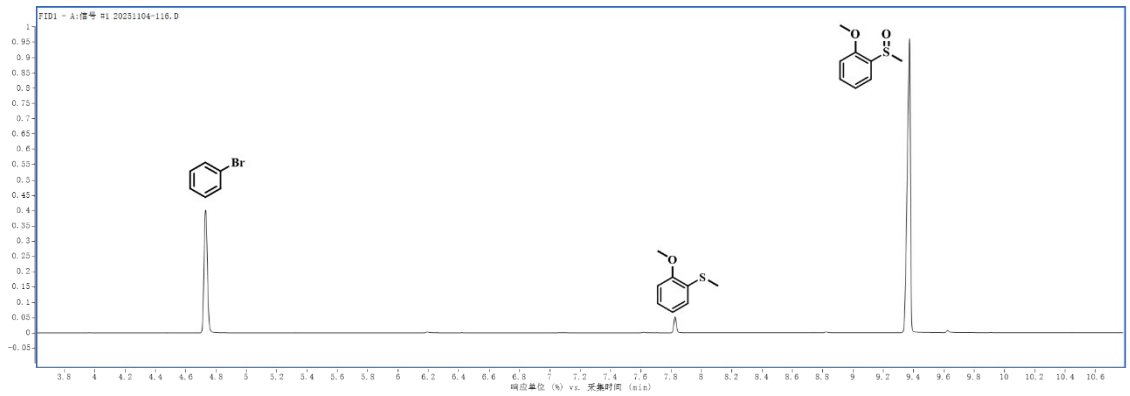

Table 1, Entry 6

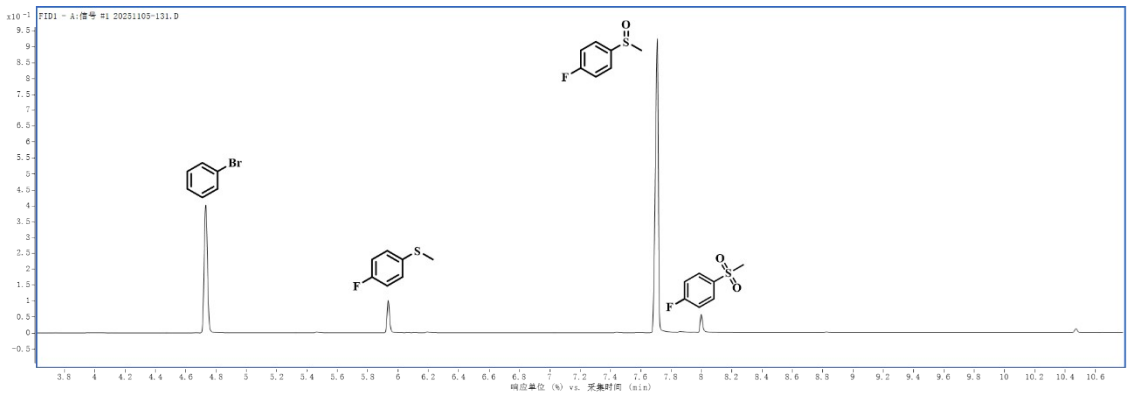

Table 1, Entry 7

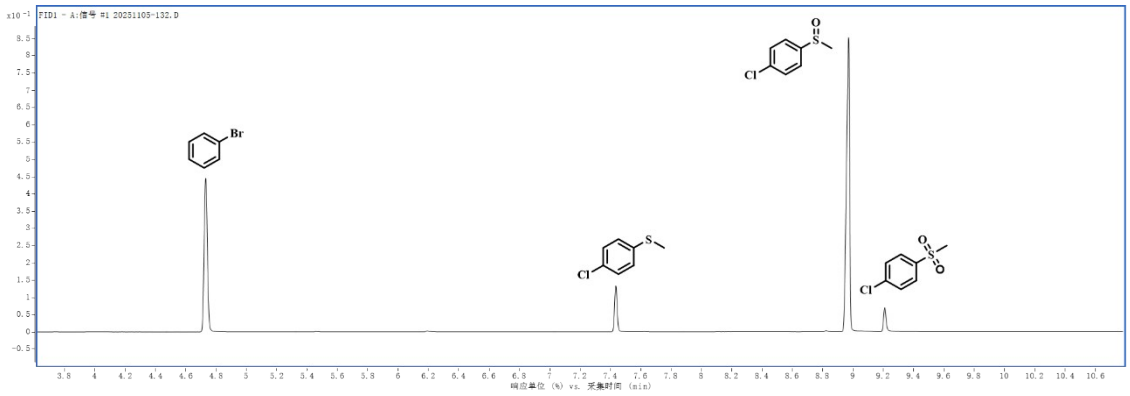

Table 1, Entry 8

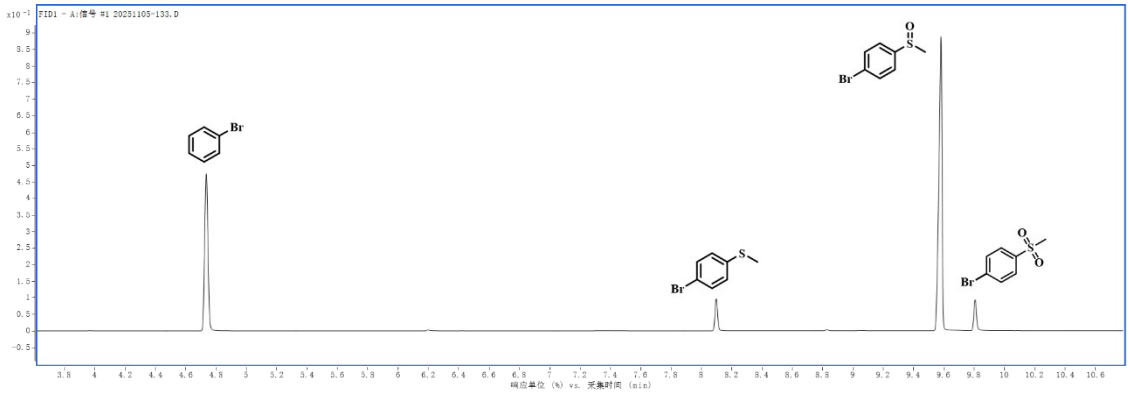

Table 1, Entry 9

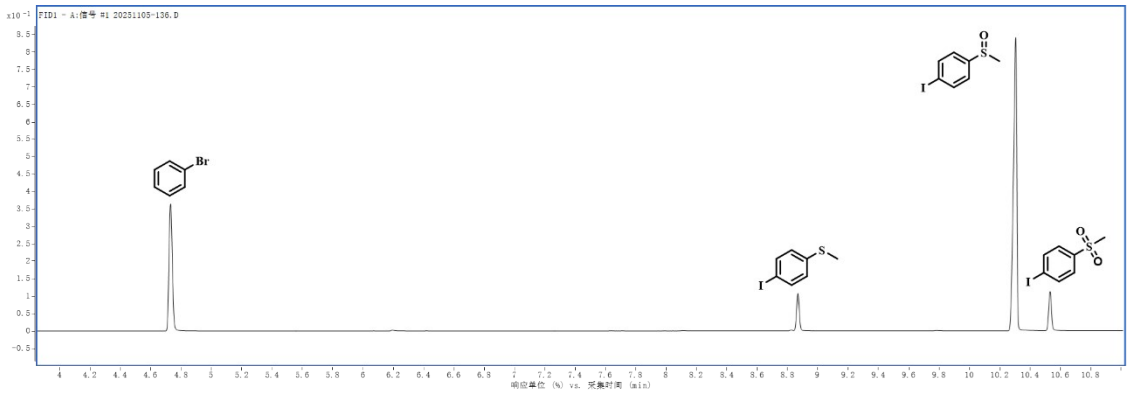

Table 1, Entry 10

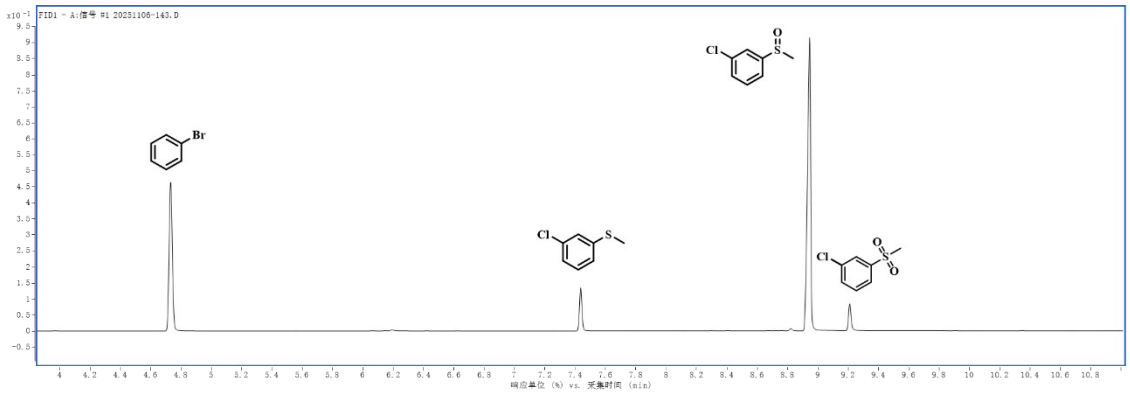

Table 1, Entry 11

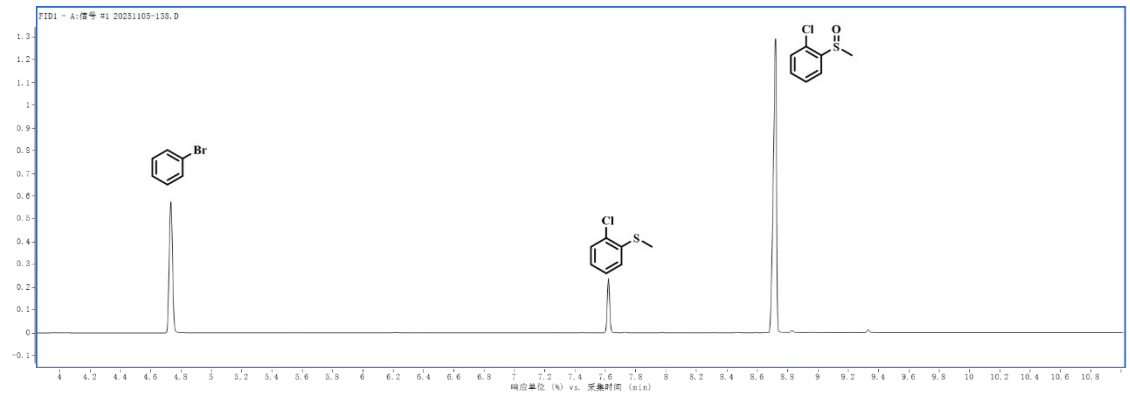

Table 1, Entry 12

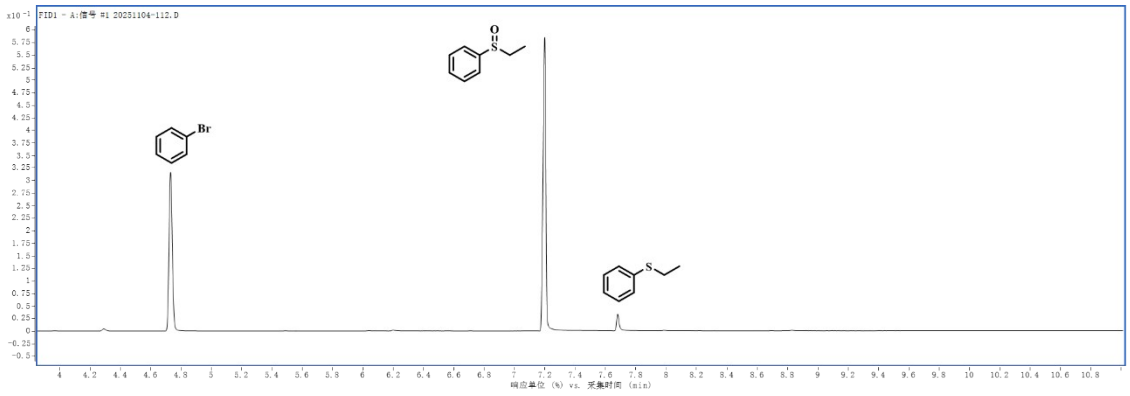

Table 1, Entry 13

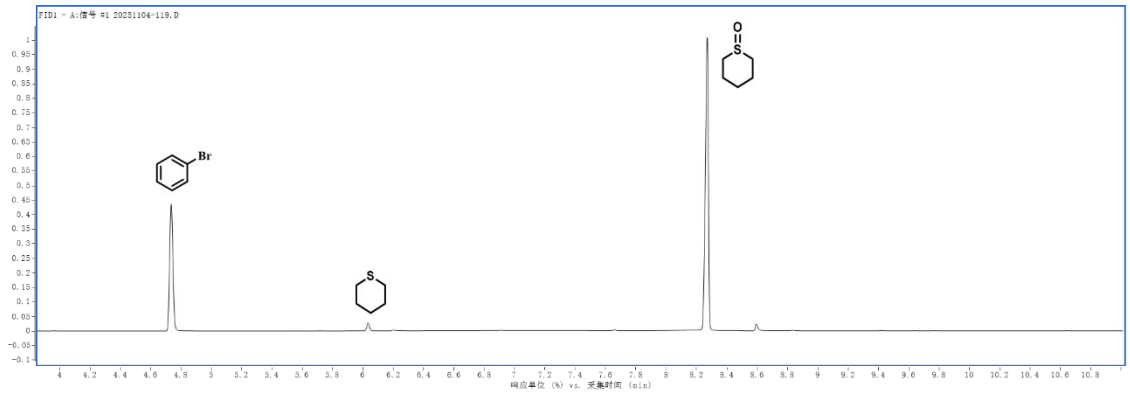

Table 1, Entry 14

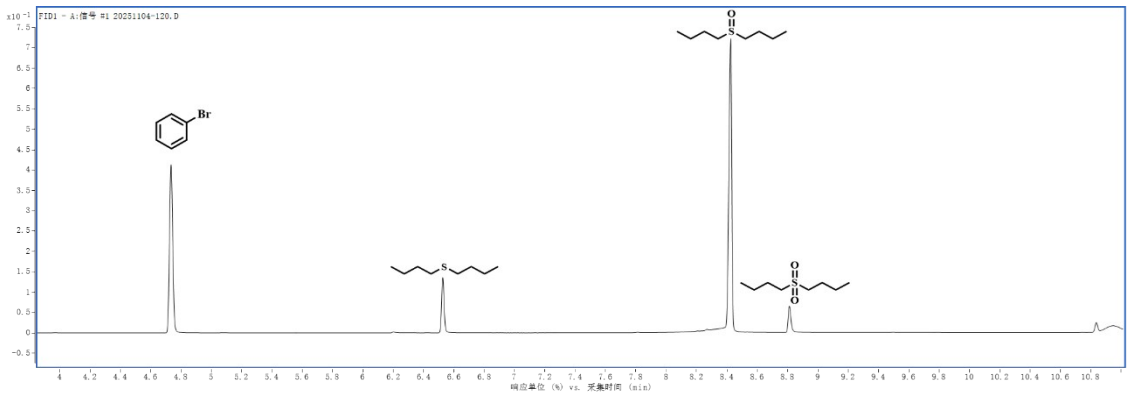

References

1. R. F. Chen, J. L. Shi, Y. Ma, G. Q. Lin, X. J. Lang and C. Wang, *Angew. Chem. Int. Ed.*, 2019, **58**, 6430-6434.
2. C. L. Su, R. Tandiana, B. B. Tian, A. Sengupta, W. Tang, J. Su and K. P. Loh, *ACS Catal.*, 2016, **6**, 3594-3599.
3. Z. J. Gu, J. J. Wang, Z. Shan, M. M. Wu, T. T. Liu, L. Song, G. X. Wang, X. H. Ju, J. Su and G. Zhang, *J. Mater. Chem. A*, 2022, **10**, 17624-17632.
4. F. Yang, X. Li, H. Y. Qu, J. L. Kan, Y. Guo and Y. B. Dong, *Chin. J. Chem.*, 2024, **42**, 1960-1966.
5. Z. H. Zhao, M. J. Liu, K. Zhou, L. D. Guo, Y. J. Shen, D. Lu, X. Hong, Z. B. Bao, Q. W. Yang, Q. L. Ren, P. R. Schreiner and Z. G. Zhang, *ACS Appl. Mater. Interfaces*, 2023, **15**, 6982-6989.
6. Q. S. Zhu, H. Y. An, T. Q. Xu, S. Z. Chang, Y. H. Chen, H. Y. Luo and Y. H. Huang, *Appl. Catal., A*, 2023, **662**, 119283.